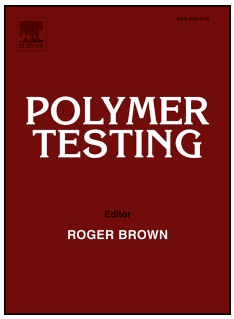

Production and characterization of elastomeric cardiac tissue-like patches for Myocardial Tissue Engineering

Sumeyye Cesur, Songul Ulag, Lara Ozak, Aleyna Gumussoy, Sema Arslan, Betul Karademir Yilmaz, Nazmi Ekren, Mehmet Agirbasli, Deepak M. kalaskar, Oguzhan Gunduz

PII: S0142-9418(20)30158-6

DOI: https://doi.org/10.1016/j.polymertesting.2020.106613

Reference: POTE 106613

To appear in: *Polymer Testing*

Received Date: 18 January 2020

Revised Date: 18 April 2020

Accepted Date: 9 May 2020

Please cite this article as: S. Cesur, S. Ulag, L. Ozak, A. Gumussoy, S. Arslan, B.K. Yilmaz, N. Ekren, M. Agirbasli, D.M. kalaskar, O. Gunduz, Production and characterization of elastomeric cardiac tissue-like patches for Myocardial Tissue Engineering, *Polymer Testing* (2020), doi: https://doi.org/10.1016/j.polymertesting.2020.106613.

Production and Characterization of Elastomeric Cardiac Tissue-like Patches for Myocardial Tissue Engineering

Sumeyye Cesur[a,b], Songul Ulag[a,b], Lara Ozak[b], Aleyna Gumussoy[b], Sema Arslan[c], Betul Karademir Yilmaz[c], Nazmi Ekren[a,d], Mehmet Agirbasli[e], Deepak M. kalaskar[f], Oguzhan Gunduz[a,g]

[a]Center for Nanotechnology & Biomaterials Application and Research (NBUAM), Marmara University, Turkey

[b]Department of Metallurgical and Materials Engineering, Institute of Pure and Applied Sciences, Marmara University, Turkey

[c]Department of Biochemistry, Faculty of Medicine, Marmara University, Turkey

[d]Department of Electrical and Electronical Engineering, Faculty of Technology, Marmara University, Turkey

[e]Department of Cardiology, Medeniyet University School of Medicine, Istanbul, Turkey

[f]UCL Division of Surgery and Interventional Science, Royal National Orthopaedic Hospital, Brockely Hill, HA7 4LP.

[g]Department of Metallurgical and Materials Engineering, Faculty of Technology, Marmara University, Turkey, 38000, 34722

ucemogu@ucl.ac.uk

Abstract

Cardiovascular disease remains the leading cause of death. Damaged heart muscle is the etiology of heart failure. Heart failure is the most frequent cause of hospital and emergency room admissions. As a differentiated organ, current therapeutics and techniques can not repair or replace the damaged myocardial tissue. Myocardial tissue engineering is one of the promising treatment modalities for repairing damaged heart tissue in patients with heart failure. In this work, random Polylactic acid (PLA), Polylactic acid/Polyethylene glycol (PLA/PEG) and random and aligned Polylactic acid/Polyethylene glycol/Collagen (PLA/PEG/COL) nanofiber patches were successfully produced by the electrospinning technique. *In vitro* cytotoxic test (MTT), morphological (SEM), molecular interactions between the components (FT-IR), thermal analysis (DSC), tensile strength and physical analysis were carried out after production. The resulting nanofiber patches exhibited beadless

and smooth structures. When the fiber diameters were examined, it was observed that the collagen doped random nanofiber patches had the lowest fiber diameter value (755 nm). Mechanical characterization results showed that aligned nanofiber patches had maximum tensile strength (5.90 MPa) values compared to PLA, PLA/PEG, and PLA/PEG/COL (random). *In vitro* degradation test reported that aligned patch had the highest degradation ratio. The produced patches displayed good alignment with tissue on cardiomyocyte cell morphology studies. In conclusion, newly produced patches have noticeable potential as a tissue-like cardiac patch for regeneration efforts after myocardial infarction.

Keywords: Collagen; Electrospinning; Myocardial tissue engineering; Polylactic acid; Polyethylene glycol.

1.Introduction

The heart is the vital organ for circulation and is composed of a complex interplay of myocardial cells with scaffolding tissue and a network of blood vessels. Arteries provide oxygen-rich blood to the cells. Heart tissue and myocardial cells require large amounts of oxygen which are provided by coronary arteries. If the coronary artery suddenly becomes occluded, the blood flow to that part of the heart is completely interrupted resulting in tissue necrosis. This condition is defined as a myocardial infarction (MI) and is the leading cause of morbidity and mortality in the developed world. Unlike other organs such as the skin or liver, the cardiac muscle's ability to regenerate itself is very limited.[1] Therefore, any damage in the heart tissue is permanent. The conversion of a healthy myocardium into non-contractile fibrous scar tissue after infarction reduces the effectiveness of cardiac contraction. Patients who survive MI frequently develop heart failure, which is defined as the clinical state resulting from the inadequacy of the heart to pump enough blood to the body's metabolic requirements. In the United States, nearly 5 million people live with heart failure. There are multiple approaches to cardiac regeneration in clinical and preclinical studies, including heart

transplant, stem cell therapy, hydrogels injection, and cardiac tissue engineering. The rapid development of tissue engineering has provided new methods for the treatment of tissue damage caused by an MI. The great achievements in stem cell technology make it possible that unlimited numbers of stem cell-derived cardiac cells could be provided for regeneration purposes.[2,3] Another novel method is the production of scaffold or patches, which support cell growth and formation of an integrated tissue or organ microenvironment.[4,5] Several parameters are considered crucial when using the patch method. These are material selection, mechanical properties, biocompatibility, surface characteristics, degradation rate, and cell seeding conditions. Nanofiber patch can be produced by a variety of methods such as self-assembly nanofibers, emulsion freeze-drying, gas foaming, solvent casting/particulate leaching, computer-aided design technology, thermally induced phase separation, and electrospinning.[6]

Electrospinning is one of the good choices to develop successful cardiovascular tissue regeneration systems. This method is common in Myocardial Tissue Engineering (MTE) and has been suggested for various biomaterials. Electrospinning is a simple, versatile fiber or nanofiber production method which uses electric force to draw charged threads of polymer solutions. In order to fabricate composite fiber with electrospinning, biomaterials like PLA, PEG, and Collagen are effective materials. Electrospun patch made of synthetic and natural polymers has been used for cardiac tissue engineering in several studies.[7–9] The biomaterials to be used for the patch for myocardium regeneration need to be compatible with the natural tissue and cells, also need to support cell adhesion, differentiation, and proliferation. Yet, the product should not compromise the elasticity of the organ. The common natural polymers used in cardiac tissue engineering include collagen, fibrinogen, chitosan, and gelatin. Natural polymers such as collagen, fibrin, and polysaccharides have shown their potential for leading to efficient cell differentiation and enhanced interaction with cardiac cells.[9] However, most

natural polymers have poor mechanical properties. Researchers have investigated the combination of collagen and synthetic polymeric materials.

Synthetic biocompatible polymers such as PLA is a solution when higher mechanical properties are required. Both materials would contribute to the patch with equal importance. The synthetic polymer would provide suitable mechanical support, whereas the natural collagen polymer would confer to the cells a more in vivo-like environment. The elastic properties of successful patch materials should be similar to those of the natural heart. The effect of these fibers that can withstand this tension during cardiac contraction and relaxation movement occurs during each heartbeat and also allows cells to attach to the structure.[10,11]

One of the preferred elastic polymers in tissue engineering is polyethylene glycol (PEG). The majority of the extracellular matrix (ECM) is collagen, which has to turn into an appropriate choice of material in cardiac tissue engineering due to its advantages such as it can provide mechanical support for the ischemic heart; improve stem cell attachment and engraftment; develop the delivery of bioactive agents for myocardial repair.[12]

In this study, the combination of biomaterials such as Collagen, PEG and PLA were used to produce nanofiber patch with therapeutic strategies using electrospinning technique which allows the production of aligned and random nanofibers by changing the rotating speed of the collector and working distance. It is known that the aligned nanofibers had enhanced mechanical properties and superior cell orientation, migration, and differentiation.[13] To provide a particular direction; mechanical, electrical, and magnetic forces have been utilized in applications. In this presented study, the electrical field was used for aligning the nanofiber patches to observe the cardiomyocyte cell direction effect on the regeneration of MI.

2. Material and Methods

2.1 Materials

Polylactic acid (PLA) 2003D was purchased from Nature Works LLC, Minnetonka, MN. Polyethylene glycol 4000 (PEG 4000) Mw=3500-4500g/mol and Collagen type I (Col) were purchased from Sigma-Aldrich. Other chemicals Acetic acid (CH_3COOH), Chloroform and Tween 80 (viscous liquid) were obtained from Sigma-Aldrich.

2.2 Preparation and characterization of electrospinning solutions

Different solutions were prepared at various concentrations and shown in Table 1. PLA granules were dissolved in 20 ml chloroform at magnetic stirring (Wise Stir®, MSH-20 A, Germany) for about 2 hrs to obtain a solution consisted of 8 wt. % at room temperature. After mixing, 3wt. % Tween 80 was added into the PLA solution and the solution was stirred for a further 15 min. Following that, different concentrations of PEG as 1, 3, and 5 wt.% added to the 8wt.% PLA solution and this mixture were stirred for 10 min. To prepare the collagen type I solution, 4 ml distilled water, 1 ml acetic acid, and 1 mg collagen were mixed for a half hour. This solution was added into the 8wt.%PLA/1wt.%PEG to obtain 8wt.%PLA/1wt.%PEG/1wt.%COL solution.

Density, electrical conductivity, surface tension, and viscosity values were measured to determine the physical characterization of the prepared electrospinning solutions. Density was measured by using a standard 10 ml bottle. The electrical conductivity was measured using the Cond 3110 SET 1, WTW, Germany. The surface tension was measured using a force tensiometer Sigma 703D, Attention, Germany. The viscosity was determined using a DV-E, Brookfield AMETEK, USA instrument. All the experiments were carried out at the ambient condition (23 ^{0}C).

2.3 Fabrication of the patches by electrospinning method

The experimental setup composes a syringe pump (NE-300, New Era Pump Systems, Inc., USA), a single brass needle (diameter of 1.63 mm), high voltage power supply connected to the needle and a laboratory-scale electrospinning unit (NS24, Inovenso Co., Turkey) (Figure

1). Polymer solutions were filled into 10 ml plastic syringes. The collector and the tip of the needle were connected to a high-voltage power supply. For electrospinning, the solutions were delivered with a constant flow rate of 3 ml/h using a syringe pump. The voltage was subjected to about 26 kV. The working distance between the needle tip and the oily paper coated circular collector was set to 170 mm. All the experiments were performed at ambient conditions (23 ^{0}C). To obtain the aligned electrospun patch, Tribot device (Origin Machine, Turkey) was used, which is available for the production of the different solutions at the same time. In this study, electrospun patches were produced at 18 kV, 12 cm distance between the collector and needle, and 4 ml/hr flow rate. Collector rotating speed was adjusted 100 revolutions per minute.

2.4 Characterization of Electrospun Patches

2.4.1 Fourier transform infrared spectroscopy (FT-IR)

Fourier-transformed infrared spectroscopy (FTIR) analysis was performed with a Jasco FT / IR-4700 model machine in order to determine the functional groups of the electrospun patches and to examine the bond structures. The measurements were carried out at room temperature (23 ^{0}C) in the transmission mode over the range 4000–400 cm $^{-1}$ and averaged over 32 scans with 4 cm^{-1} resolution. Know-it-all software was used to analyze spectrums.

2.4.2 Scanning electron microscopy (SEM)

The morphological characterization of electrospun patches was investigated using a Scanning Electron Microscope (SEM, EVO LS 10, ZEISS). Before imaging, samples were sputter-coated with gold-palladium for 120 s using a Quorum SC7620 Mini Sputter Coater. The applied accelerating voltage was 10 kV. The average fiber diameter and their distribution were measured by using image software (Olympus AnalySIS, USA).

2.4.3 Mechanical properties

Before the tests, each different sample was sectioned into five rectangular-shaped samples which are 5 cm in length and 1 cm in width. The thickness of each tensile test specimen was measured using a high-accuracy digital micrometer (Mitutoyo, USA). The tensile strength and strain of electrospun patches were performed using a tensile tester (Shimadzu, Japan) by means of running special software. All samples were subjected to test the speed of 5 mm/min until the breaking point at room temperature (23 ^{0}C).

2.4.4 Differential scanning calorimetry analysis (DSC)

The thermal properties such as melting temperatures (T_m) and glass transition temperatures (T_g) of the electrospun patches were examined by using a differential scanning calorimeter (DSC) (Shimadzu, Japan). Temperature ranges were adjusted from 25 ^{0}C to 100 ^{0}C for all patches and the heating rate was selected as 10 ^{0}C/min.

2.4.5 *In vitro* degradation test

Since the 8%PLA/1%PEG, 8%PLA/1%PEG/1%COL random, and 8%PLA/1%PEG/1%COL aligned patches had high viability values in cell culture test, the degradation behaviour of these patches were tested to examine the mass change effect in cell viability values. *In vitro* degradation behavior was evaluated in a phosphate-buffered salline (PBS, pH=7.4) for a week and measurements were taken every day. During the degradation test, PBS was changed every measurement to provide fresh PBS to the patches. Equation 2.4.5.1 was used to calculate the weight loss (W_L) of the patches in PBS. In this equation W_0 is the initial weight and W_d is the dried weight of the patches.[14]

$$W_L = \frac{W_0 - W_d}{W_0} . 100 \qquad (2.4.5.1)$$

2.4.6 MTT Cytotoxicity Assay

H9C2 cell is a human cardiomyocyte cell line purchased from the American Type Culture Collection (from ATCC). Cells were cultured in complete Dulbecco's Modified Eagle Medium (DMEM) supplemented with 10% fetal bovine serum (FBS), 1%

Penicillin/Streptomycin and incubated at 37 ° C and 5% CO_2. To examine cell viability on both non-degradable and degraded patches; materials were cut and put to 24 well plates and sterilized with UV. They were incubated at 37 ° C and 5% CO_2 in 1 ml of 10% fetal bovine serum (FBS), 1% Penicillin/Streptomycin supplemented with DMEM at $20x10^3$ cells per well. The medium was added daily (500 µL). MTT protocol: Cell viability was measured using MTT reagent (Sigma) dissolved in PBS (5 mg/ml). 100 µL is taken from this parent stock and seeded on cells and materials in DMEM supplemented with 10% FBS, 1% Penicillin/Streptomycin and incubated for 3 hours at 37 ° C and 5% CO_2. DMEM was withdrawn from the cell-medium and formazan crystals were dissolved in 500 µL DMSO solution, followed by 4 replicates in 96 well-plates, measured by light absorbance at 570 nm.

H9C2 cell was cultured at $20x10^3$ cells/cm^2 on the nanofiber patches in the 24 well plate for the F-actin staining. Firstly, H9C2 proliferation on the nanofiber patch was performed for a period of 4 days, after that the F-actin staining kit (Abcam, CytoPainter F-actin Labeling Kit) was carried out to examine the cell phenotype according to manufacturer standard. Initially, the cells were fixed with 4% formaldehyde (Sigma) at room temperature for 15 min. Then, they were washed and incubated with 0.1 % Triton X-100 (Merck) to enhance permeability for 10 minutes. The cells and green fluorescent phalloidin conjugates were incubated together for 1 h at room temperature. Then, the cell-nanofiber patches were washed with PBS and incubated with DAPI (Invitrogen) (1:5000) for 10 min to stain the nuclei. Before mounting on a glass slide, patches were washed with PBS and they were visualized under laser scanning confocal microscopy (LSM 700, Zeiss).

3. Results and Discussions

3.1 Physical characterization of the polymer solutions

The physical properties of electrospinning solutions such as density, surface tension, electrical conductivity, and viscosity are one of the most important parameters affecting the spinning

process.[15] These parameters have been observed to affect electrospun polymer fiber homogeneity and nanofiber formation.[16] For example, electrical conductivity and viscosity are the parameters that affect fiber diameters most. Electrical conductivity is very important for the structure of the fibers produced.[17] Since solutions with high electrical conductivity are known to have a reducing effect on fiber diameters.[18,19] Physical properties of solutions used in electrospinning are shown in Table 2. By the addition of different amounts of PEG into the PLA, it was observed that PEG affects the viscosity parameters reversely.[20,21] Although small amounts of Collagen I were added to 8%PLA/1%PEG, sharp increases in electrical conductivity were observed.[22] As a result, the presence of the collagen positively affected the electrical conductivity of the nanofiber patches, because collagen had good electrical conductivity. In addition to this result, it has been reported in previous studies that Tween-80, an amphiphilic, nonionic, non-toxic surfactant, improves the spinnability and high homogeneity of fibers by adding to spinning solutions.[23,24]

3.2 Fourier transform infrared spectroscopy (FT-IR)

FTIR analysis was carried out to investigate the functional groups of electrospun nanofiber patches (Figure 2). PLA related infrared spectra were observed in the curve of PLA, PLA-PEG and PLA-PEG-Collagen nanofiber patches. Figure 2 (a), collagen characteristic amide peaks: Amide I observed at~1627 cm^{-1} due to the υ(C=O) vibrations, ~1336-1450 cm^{-1} are due to the δ(CH_3), δ(CH_2) stretching and υ(C- N), δ(N- H) absorption bands of amide III (~1235 cm^{-1}).[25] Figure 2 (b), PEG characteristic infrared bands were observed C□H stretching at 2890 cm^{-1} and the C□O (ether) stretching at 1125 cm^{-1}.[26] Figure 2 (c), PLA the main absorption peaks were observed C=O vibration peak at 1749 cm^{-1}, CH_3 asymmetrical scissoring at 1453 cm^{-1}, C–O, C–O–C stretching at 1080 cm^{-1}, C–CH_3 stretching at 1042 cm^{-1} and C–COO stretching peak at 867 cm^{-1}.[27] Since the amount of PLA was high, the added materials caused very little shifts.

3.3 Morphological characterization of patches

Scanning Electron Microscopy (SEM) was used to understand the morphology of the nanofiber patches produced. The diameters of each sample were measured. SEM images and diameters of the prepared nanofiber patches are given in Figure 3, which demonstrated the morphology of the random and aligned nanofiber patches and their corresponding diameter distribution. Highly uniform and smooth nanofiber were formed without the occurrence of bead defects for all the random and aligned nanofiber patches. It was observed that nanofiber patches' diameters increased when PEG was added in different ratios. The results found in this study have been presented in previous studies.[28-30] The mean nanofiber diameters were 1472±534 nm, 1569±253 nm, 1665±267 nm and 1881±401 nm corresponding to the PLA, PLA/PEG ratio of 8/0, 8/1, 8/3 and 8/5 respectively.

The nanofiber diameter decreased sharply with adding of 1wt. % Collagen into the 8% PLA/1%PEG. A possible explanation is that this situation might be due to the high electrical conductivity of collagen.[21] Furthermore, the random and aligned nanofiber patches had the mean fiber diameters, which were 752±142 nm, 1006±281 nm, respectively. Compared with the random and aligned nanofiber patches, the aligned nanofibers possessed a larger diameter due to the voltage and working distance differences between them which were 18kV, 12 cm for aligned and 26kV, 17 cm for random nanofiber patches.

3.4 Mechanical examination of the patches by Tensile Testing

The tensile properties of all nanofiber patches were investigated at room temperature, as shown in Table 3 with values of tensile strength and elongation at break (%). Such results are crucial in determining the elasticity of the product. The neat PLA had the lowest strain value compared to the other nanofiber patches. This situation was the typical result for PLA which has a rigid and brittle structure. Its tensile strength was high, but with limited and low elongation at break.[31] By the addition of the PEG into the 8%PLA, strain values were

increased however tensile strength values were decreased except for 8%PLA/1%PEG nanofiber patch which had the minimum PEG content.[20, 32] This result revealed that with the increase of the strain at break, and the brittleness of PLA decreased indicated that elongation and brittleness are inversely proportional to each other. [31] Another important result was that the tensile strength values of the aligned nanofiber patch were higher than the random nanofiber patch. This result showed that aligned nanofibers had a constitutional tensile strength in the direction of alignment. [33] The reason for low tensile strength and strain at break values of random nanofiber patch compared to those values of aligned nanofiber patch that random nanofiber had a highly porous structure which could be a negative effect on mechanical properties. [34]

3.5 Differential Scanning Calorimetry (DSC)

Thermal transition temperatures affect the physical characteristics of PLA, such as density, heat capacity, and rheological measurements. Depending on the thermal properties, PLA can be amorphous or semi-crystalline in the solid state. Glass transition temperature is an important parameter for determining the upper use temperature of PLA for commercial applications.[35] In Figure 4, it was observed only the single glass transition temperature peak for all patches. This might be due to the effective interactions and distributions between the polymers, there no phase separation observed. Glass transition temperatures for 8%PLA, 8%PLA/1%PEG, 8%PLA/3%PEG, 8%PLA/5%PEG, 8%PLA/1%PEG/1%COL, patches were 56, 59, 57, 57, and 53 °C, respectively. The glass transition temperature of 8%PLA/1%PEG/1%COL was lower compared to 8%PLA and other patches. The 8%PLA/1%PEG patch had a maximum glass transition temperature value. By the addition of more PEG into 8%PLA, glass transition temperature value shifted to higher temperatures.[36]

3.6 *In vitro* degradation behaviours of the nanofiber patches

In vitro degradation study was carried out to determine the behaviour of the patches in the aqueous environment. In Figure 5, all nanofiber patches showed swelling behaviour after 24 h

incubation. 8%PLA/1%PEG/1%COL aligned patch had the highest swelling ratio (602%) between them. The lowest swelling ratio (313%) was observed for the sample of 8%PLA/1%PEG. On the second day, the swelling ratio of 8%PLA/1%PEG/1%COL random patch continued to increase. On the third day, degradation ratios of all the nanofiber patches decreased and this behavior continued for other days up to seventh days of incubation time. When the one-week incubation was evaluated, it was seen that initially the patches absorbed the PBS and then mass loss was started for all patches. Maximum degradation ratio was seen for 8%PLA/1%PEG/1%COL aligned patch and 8%PLA/1%PEG patch had the least degradation ratio. Since the swelling ratio of the 8%PLA/1%PEG/1%COL aligned patch was high, its degradation ratio was also fast to decompose.[37]

3.7 Cell viability results of the patches

The cell viability of nanofiber patches was examined for 1, and 3 days after seeding and results were shown in Figure 6a. Cell viability values of patches after 1-day incubation were lower than the control group (H9C2 cell). Maximum viability observed for the aligned patch for 1-day incubation. On 3rd day, it was found a significant increase in the viability values of the patches containing collagen. Especially, the aligned patch had a maximum cell viability value (143%), this gave a 43% difference compared to the control group (%100). Another result of the cell viability test was that cell viability was very low by adding more PEG into the 8%PLA. In Liu et al. was found that at high concentrations, PEG-1000, PEG-4000, and mPEGMA-950 exhibited moderate cytotoxicity. [38]

The cell viability of degraded nanofiber patches (8%PLA/1%PEG, 8%PLA/1%PEG/1%COL random, 8%PLA/1%PEG/1%COL aligned), was also performed to examine the mass change effect on the viability for 1, and 3 days incubation. In Figure 6b, it was observed 38% decrease in cell viability for 8%PLA/1%PEG nanofiber patch after 1 day incubation and 15% decrease after 3 days incubation period. However, it was seen that the patches which have

collagen protein displayed an increasing behaviour in cell viability for 1 and 3 days incubation time. On day 1, the difference between the viability values before and after degradation was 229% for the 8%PLA/1%PEG/1%COL random nanofiber patch. On day 3, it was found that the difference was 77%. On the other hand, no significant increase in cell viability values of 8%PLA/1%PEG/1%COL aligned patches before and after degradation was observed. The differences were 28% and 1.8% for 1 and 3 days incubation, respectively for aligned patch. When the viability values of the non-degradable and degraded nanofiber patches were compared, it was concluded that only 8%PLA/1%PEG nanofiber patch showed a decrease in cell viability. Other patches had a notable increase in the viability values during the incubation period. The reason for this behavior can be explained as both 8%PLA/1%PEG/1%COL random and 8%PLA/1%PEG/1%COL aligned patches had high degradation ratios which can improve the survival of the cells.[39]

To observe the distribution of cells on the nanofiber patches, the confocal microscope was used. Figure 7 showed the confocal images of the 8%PLA/1%PEG/1%COL random and aligned patches with their scale bars. After 4 day incubation, nuclei were seen with phenotypes for two patches. In Figure 7a, it can be said that cells on the patches also had random distribution. However, for aligned patches in Figure 7b, it can be said that cells had nearly aligned arrays throughout the aligned patch. This alignment can be more obvious after 7 days culture period and cell morphology can be changed. [40] However, this confocal image showed the difference between the random and aligned nanofiber patches. It can be deduced from is that aligned patch has the capacity to array the cells.

3.7 Cell adhesion and growth on patches

The produced patch materials should be suitable for cell attachment and proliferation in order to get a functional cell network. The morphology of H9C2 cells on patches was investigated by SEM for 8%PLA/1%PEG and 8%PLA/1%PEG/1%COL random, and

8%PLA/1%PEG/1%COL aligned patches. The aim was to differentiate the characteristics of cell attachment and growth between the random and aligned patches. As shown in Figure 8, cells spread on scaffolds effectively after 3 days of incubation. As Figure 8 (a, b) indicate, cells on 8%PLA/1%PEG were attached to each other, and formed large clumps instead of spreading on the patches.[41] In Figure 8 (c, d), 8%PLA/1%PEG/1%COL random patch with homogeneous, broad cell attachment showed spread geometry.[42] Figure 8 (e, f) showed the SEM images of 8%PLA/1%PEG/1%COL aligned patch with cell attachment. It was seen that H9C2 cells on the aligned patches were spread along the nanofiber direction. The cells were oriented as desired on the aligned structured nanofibers and connect with each other along an aligned line.[43] It can be deduced from those aligned patches had better cell guidance than random patches. However, it should be noted that all patches improved cell growth and attachment efficaciously. In particular, the cell attachment results showed that collagen is both responsible for the strength and alignment of cardiomyocytes and also responsible for the myocardial hardness. [44]

Conclusions

Myocardial regeneration is an attractive target for tissue engineering. In the present study, random and aligned nanofiber patches by using Polylactic acid (PLA) Polyethylene glycol (PEG) and Collagen were fabricated through electrospinning. It was observed that viscosity decreases as PEG are added to PLA in different ratios. A significant increase in electrical conductivity was observed after adding even a small amount of collagen to %8 PLA%1 PEG (wt). With the addition of collagen, fiber diameter was reduced in both random and aligned nanofiber patches. The lowest fiber diameter (752 nm) was observed in the random sample containing collagen. With PEG addition into the PLA with various amounts, it was reported that PEG increased the glass transition temperature of the neat PLA. However, collagen addition decreased the glass transition temperature by about 3°C. Another important result

was that the tensile strength of aligned nanofiber patches had the maximum value. The 8%PLA/1%PEG, 8%PLA/1%PEG random, and 8%PLA/1%PEG aligned patches were tested in PBS for 7 days incubation time and cell studies performed again for these patches to observe the mass change effect on the viability values. Cell viability before and after degradation test and proliferation studies displayed promising findings. Random and aligned patches show the therapeutic potential of myocardial repair and tissue engineering. Most importantly, aligned patches had a maximum cell viability rate. Cardiomyocyte cells grow on the aligned patches homogeneously. The newly designed and developed patch shows promising characteristics *in vitro* models.

Acknowledgements

This study supported financially by FEN-C-YLP-101018-0539 project.

References

1 R. Zak, *Amer.Heart Ass.Monogr., 1974, **35,** 17-26.*

2 P. Bianco and P. G. Robey, *Nature.*, 2001, **414**, 118.

3 A. Jaklenec, A. Stamp, E. Deweerd, A. Sherwin and R. Langer, *Tissue Eng. - Part B Rev.*, 2012, **18**, 155–166.

4 L. G. Griffith and G. Naughton, *Science,* 2002, **295**, 1009.

5 S. F. Badylak, D. J. Weiss, A. Caplan and P. MacChiarini, *Lancet*, 2012, **379**, 943–952.

6 A. Tmayol, M. Akbari, N. Annabi, A. Paul, A. Khademhosseini and D. Juncker, *Biotechnol. Adv.*, 2013, **31**, 669-687.

7 S. Mukherjee, C. Gualandi, M. L. Focarete, R. Ravichandran, J. R. Venugopal, M. Raghunath and S. Ramakrishna, *J. Mater. Sci. Mater. Med.*, , DOI:10.1007/s10856-011-4351-2.

8 P. H. Kim and J. Y. Cho, *BMB Rep.*, 2016, **49**, 26-36.

9 M. Kitsara, O. Agbulut, D. Kontziampasis, Y. Chen and P. Menasché, *Acta Biomater.*,

2017, **48**, 20–40.

10 T. C. McDevitt, K. A. Woodhouse, S. D. Hauschka, C. E. Murry and P. S. Stayton, *J. Biomed. Mater. Res. - Part A*, 2002, 586–595.

11 R. K. Iyer, L. L. Y. Chiu and M. Radisic, *J. Biomed. Mater. Res. - Part A*, 2006, **40**, 877.

12 W. Wu, S. Peng, Z. Song, S. Lin, *Drug Delivery and Translational Research*, 2019, 9, 920–934.

13. N. Mohan and M. S. Detamore, in *Nanotechnology Applications for Tissue Engineering*, 2015, 57-75.

14 FH. Zulkifli, F. S. J. Hussain, M. S. B.A. Rasad, M. M. Yusoff, *Polymer Degradation and Stability*, 2014, 110, 473-481.

15. H. W. Kwak, M. Shin, J. Y. Lee, H. Yun, D. W. Song, Y. Yang, B. S. Shin, Y. H. Park and K. H. Lee, *Int. J. Biol. Macromol.*, 2017, **102**, 1092–1103.

16 S. Tan, R. Inai, M. Kotaki and S. Ramakrishna, *Polymer.* 2005, **46**, 6128–6134.

17 C. Mit-Uppatham, M. Nithitanakul and P. Supaphol, *Macromol. Chem. Phys.*, 2004, **205**, 2327-2338.

18 T. Jarusuwannapoom, W. Hongrojjanawiwat, S. Jitjaicham, L. Wannatong, M. Nithitanakul, C. Pattamaprom, P. Koombhongse, R. Rangkupan and P. Supaphol, *Eur. Polym. J.*, 2005, **41**, 409.

19 R. Konwarh, N. Karak and M. Misra, *Biotechnol. Adv.*, 2013, **31**, 421.

20 M. Bijarimi, S. Ahmad, R. Rasid, M. A. Khushairi and M. Zakir, in *AIP Conference Proceedings*, 2016. DOI:10.1063/1.4945957

21 E. Hendrick and M. Frey, *J. Eng. Fiber. Fabr.*, 2014, **9,** 153-164.

22 M. O. Aydogdu, J. Chou, E. Altun, N. Ekren, S. Cakmak, M. Eroglu, A. A. Osman, O. Kutlu, E. T. Oner, G. Avsar, F. N. Oktar, I. Yilmaz and O. Gunduz, *Int. J. Polym.*

Mater. Polym. Biomater., 2019, **68**, 243-255.

23 R. Rošic, P. Kocbek, S. Baumgartner and J. Kristl, *J. Drug Deliv. Sci. Technol.*, 2019, **21**, 229–236

24 S. Q. Wang, J. H. He and L. Xu, *Polym. Int.*, 2008, 57, 1079–1082.

25 C. Mahapatra, G. Z. Jin and H. W. Kim, *Tissue Eng. Regen. Med.*, 2016, **13**, 538–546.

26 R. Patel and M. Patel, *J. Dispers. Sci. Technol.*, 2008, **29**, 193–204.

27 S. Cesur, F. N. Oktar, N. Ekren, O. Kilic, D. B. Alkaya, S. A. Seyhan, Z. R. Ege, C.-C. Lin, S. E. Kuruca, G. Erdemir and O. Gunduz, *J. Aust. Ceram. Soc.*, 2019, 1–11.

28 M. Spasova, O. Stoilova, N. Manolova, I. Rashkov and G. Altankov, *J. Bioact. Compat. Polym.*, 2007, **22**, 62-76

29 S. J. Reinholt, A. Sonnenfeldt, A. Naik, M. W. Frey and A. J. Baeumner, *Anal. Bioanal. Chem.*, 2014, **406**, 3297–3304.

30 N. C. Nepomuceno, M. A. Barbosa, R. F. Bonan, J. E. Oliveira, F. C. Sampaio and E. S. Medeiros, *J. Appl. Polym. Sci.*, 2018, **135**, 9

31 B. W. Chieng, N. A. Ibrahim, W. M. Z. Wan Yunus and M. Z. Hussein, in Advanced Materials Research, 2014, 6, 93-104.

32. A. K. Mohapatra, S. Mohanty and S. K. Nayak, Polym. Compos., 2014, 35, 283-293.

33. H. Y. Lin, W. C. Tsai and S. H. Chang, J. Biomater. Sci. Polym. Ed., 2017, 28, 664-678.

34. A. Doustgani, E. Vasheghani-Farahani, M. Soleimani and S. Hashemi-Najafabadi, Int. J. Nanosci. Nanotechnol., 2011, 7, 127–132.

35. L. T. Sin, A. R. Rahmat and W. A. W. A. Rahman, in Handbook of Biopolymers and Biodegradable Plastics: Properties, Processing and Applications, 2012, 55-69.

36. J. Ren, H. Hong, T. Ren and X. Teng, *React. Funct. Polym.*, 2006, **66**, 944–951.

37 D. Wang, D. J.T. Hill, H. Peng, A. Symons, S. Varanasi, A. K. Whittaker, F. Rasoul, *Macromol. Symp.*, 2010, 296, 233–237.

38. G. Liu, Y. Li, L. Yang, Y. Wei, X. Wang, Z. Wang and L. Tao, *RSC Adv.*, 2017, **7**, 18252-18259.

39. J. Yi, F. Xiong, B. Li, H. Chen, Y. Yin, H. Dai, S. Li, *Regen Biomater.*, 2016, 3.

40. M. Khan, Y. Xu, S. Hua, J. Johnson, A. Belevych, Paul M, L. Janssen, S. Gyorke, J. Guan, M. G. Angelos, PLOS ONE, 2015.

41. Y. Ganji, Q. Li, E. S. Quabius, M. Böttner, C. Selhuber-Unkel and M. Kasra, *Mater. Sci. Eng. C*, 2016, **59**, 10-18.

42 B. Çelebi Saltik and M. Ö. Öteyaka, *Turkish J. Biol.*, 2016, 40, 510-518.

43 D. Kai, M. P. Prabhakaran, G. Jin and S. Ramakrishna, *J. Biomed. Mater. Res. - Part B Appl. Biomater.*, 2011, **98**, 379-386.

44 B. W. Chieng, N. A. Ibrahim, W. M. Z. Wan Yunus and M. Z. Hussein, in *Advanced Materials Research*, 2014, **6**, 93-104.

Table 1. Content table of solution samples.

Nanofiber Patches	PLA content (Wt %)	PEG content (Wt %)	COL content (Wt %)	Tween 80 (Wt %)
8PLA	8	0	0	3
8PLA/1PEG	8	1	0	3
8PLA/3PEG	8	3	0	3
8PLA/5PEG	8	5	0	3
8PLA/1PEG/1COL (Random)	8	1	1	3
8PLA/1PEG/1COL (Aligned)	8	1	1	3

Table 2. Physical characterization of solutions used before the electrospinning process.

Concentration of Solutions	Density (g/cm^3)	Electrical Conductivity (µS/cm)	Surface Tension (mN/m)	Viscosity (mPa.s)
8 wt. % PLA	1.400	1.2	28.54	56
8 wt. % PLA 1 wt.% PEG	1.488	0.8	29.01	732
8 wt. % PLA 3 wt.% PEG	1.478	0.9	29.45	644
8 wt. % PLA 5 wt.% PEG	1.470	1.0	29.67	625
8 wt. % PLA 1 wt. % PEG 1 wt.% COL	1.409	64.1	29.46	580

Table 3. Tensile test measurement results of nanofiber patches.

Nanofiber Patches	Tensile strength (MPa)	Strain at break (%)
8wt.%PLA	0.24 ± 0.06	61.17 ±0.74
8wt.%PLA/1 wt.%PEG	0.25 ± 0,03	142.48 ± 17.1
8 wt.%PLA/3 wt.%PEG	0.11 ± 0.008	187.89 ± 4.02
8 wt.%PLA/5 wt.% wt.%PEG	0.10 ± 0.02	192.56 ± 8.47
8wt.%PLA/1wt.%PEG/1 wt.%COL (Random)	0,11 ± 0.01	72,13 ± 2.46
8wt.%PLA/1wt.%PEG/1 wt.%COL (Aligned)	5.90 ± 4.00	84.08 ± 11.76

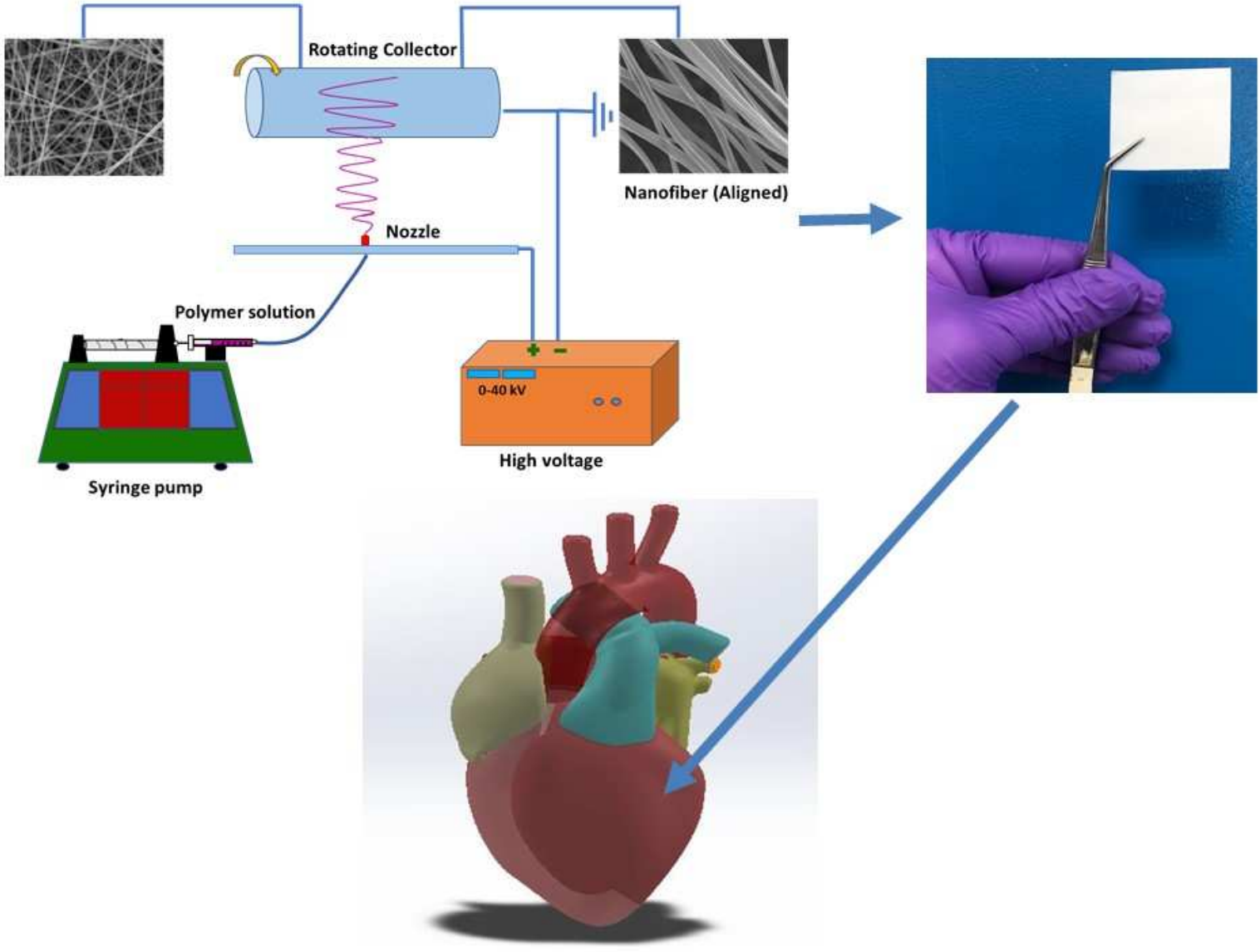

Figure 1. Schematic images of the nanofiber patches produced by the electrospinning method.

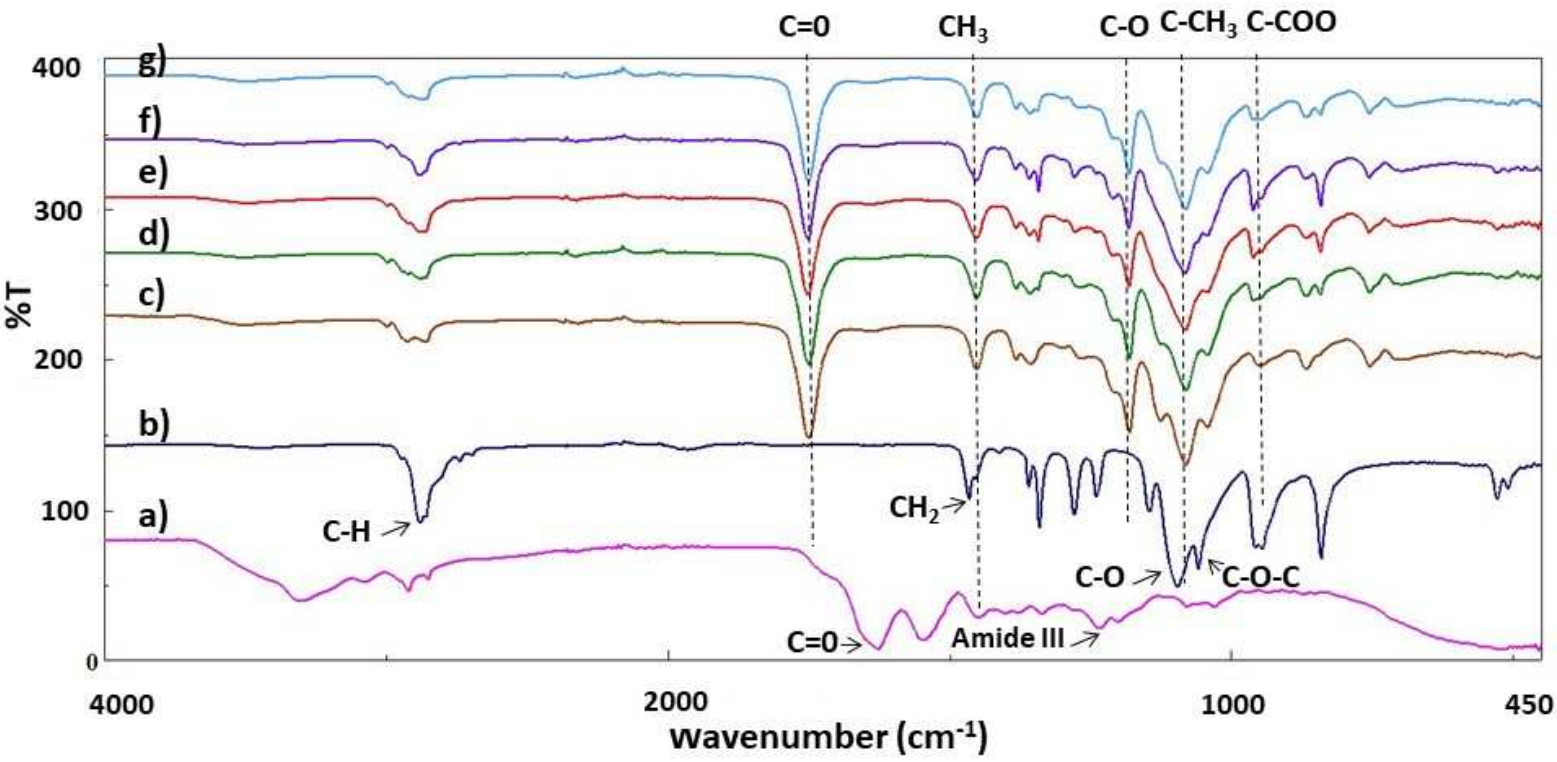

Figure 2. FTIR Spectra of the nanofiber patches.

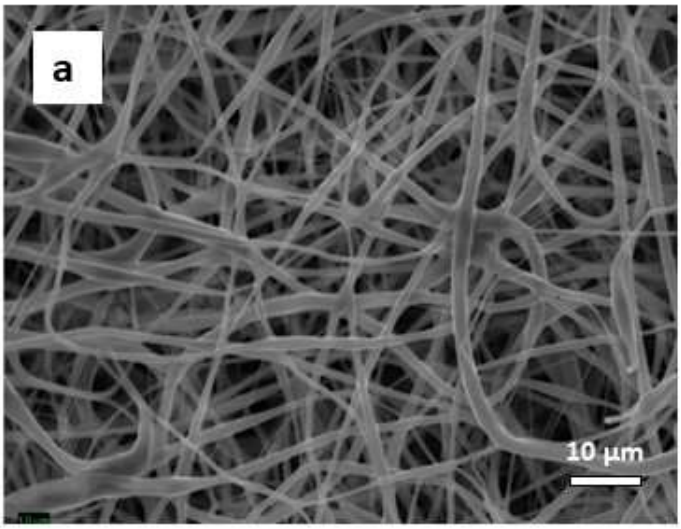
a
10 µm

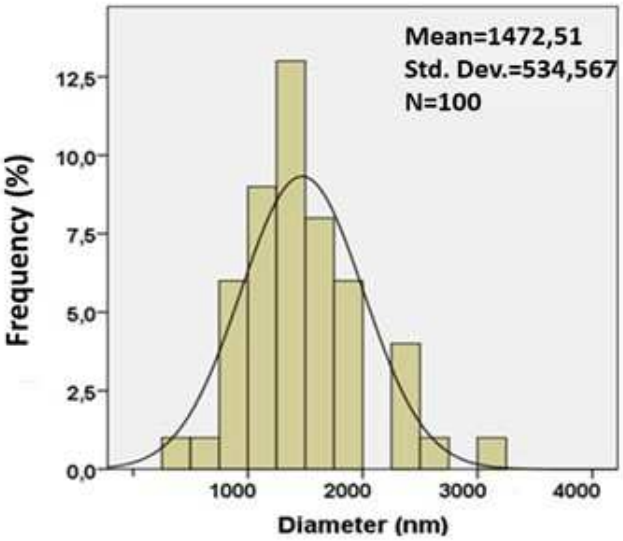
Mean=1472,51
Std. Dev.=534,567
N=100
Frequency (%)
12,5
10,0
7,5
5,0
2,5
0,0
1000
2000
3000
4000
Diameter (nm)

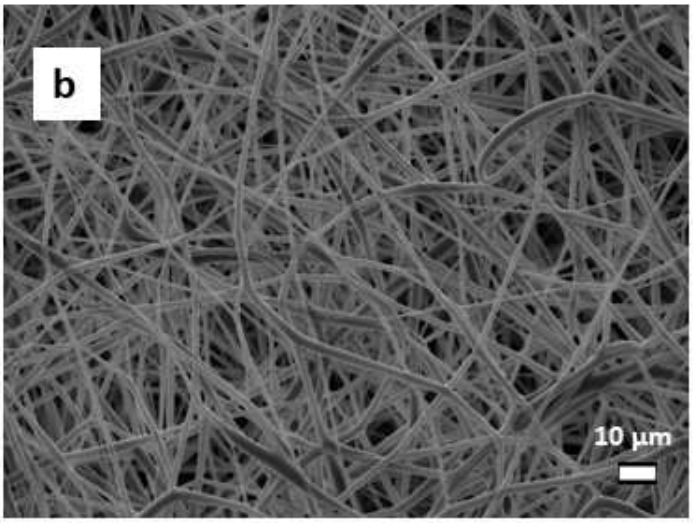
b
10 µm

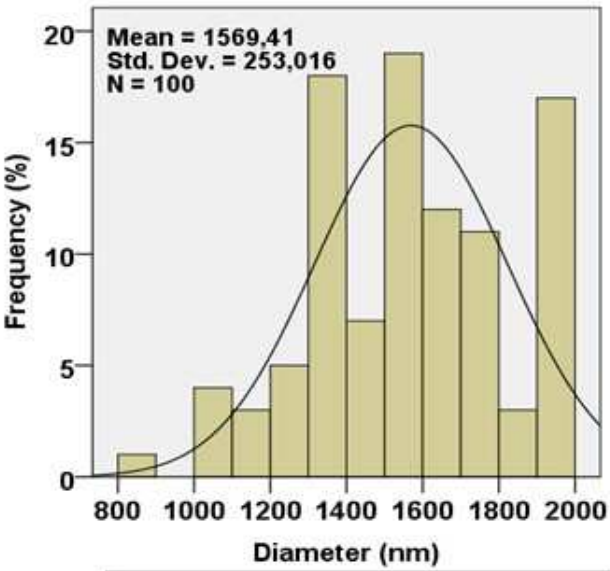
Mean = 1569,41
Std. Dev. = 253,016
N = 100
Frequency (%)
20
15
10
5
0
800
1000
1200
1400
1600
1800
2000
Diameter (nm)

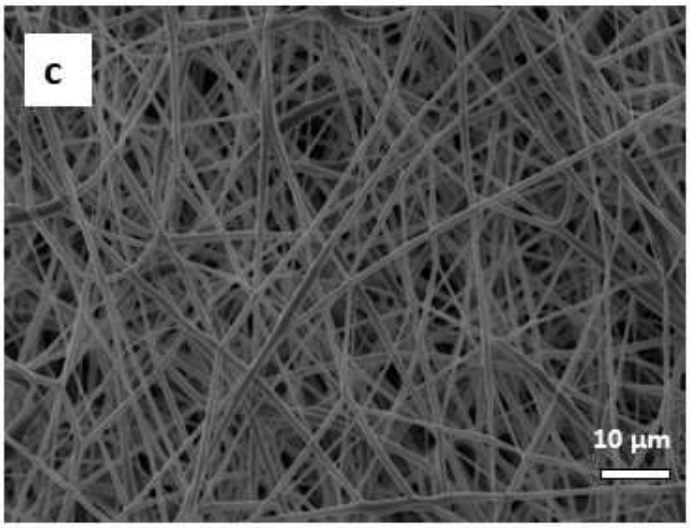
c
10 µm

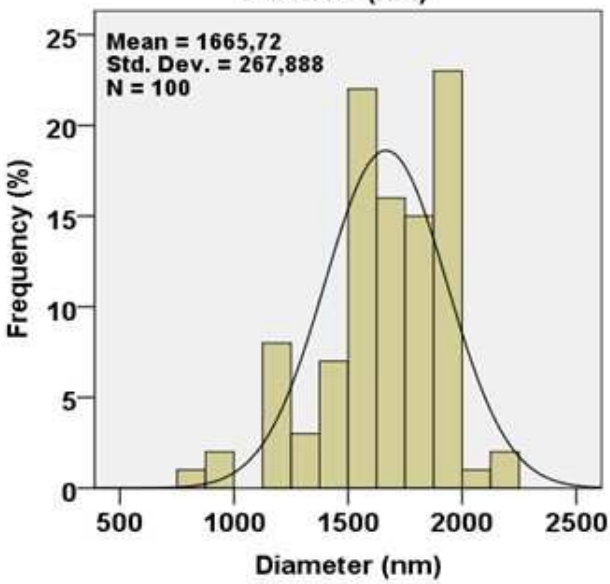
Mean = 1665,72
Std. Dev. = 267,888
N = 100
Frequency (%)
25
20
15
10
5
0
500
1000
1500
2000
2500
Diameter (nm)

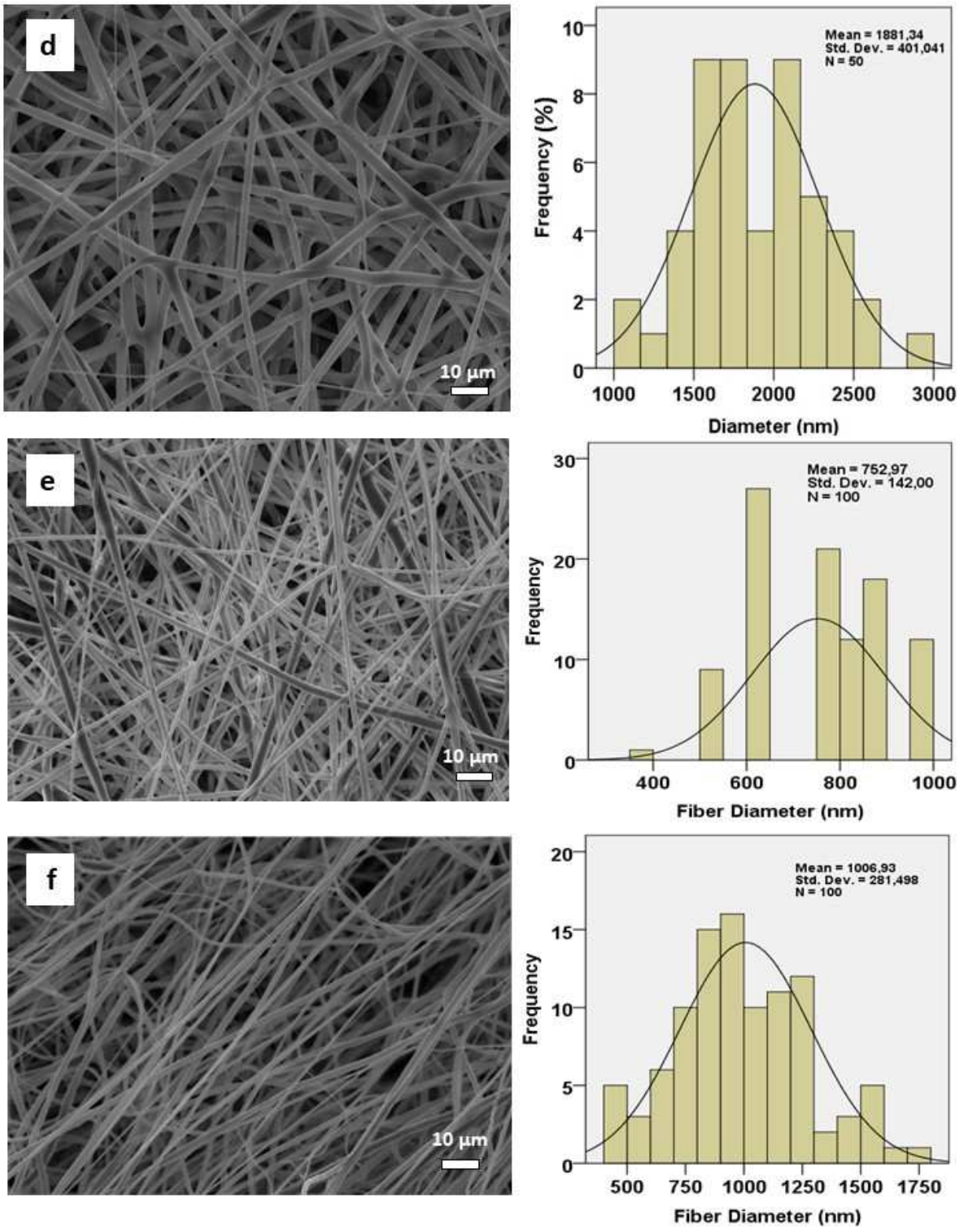

Figure 3. Scanning electron microscopy images and fiber diameter distribution of nanofiber patches: 8 %PLA (a), 8%PLA/1%PEG (b), 8%PLA/3%PEG (c), 8%PLA/5%PEG (d), random 8%PLA/1%PEG/1%COL (e), aligned 8%PLA/1%PEG/1%COL (f).

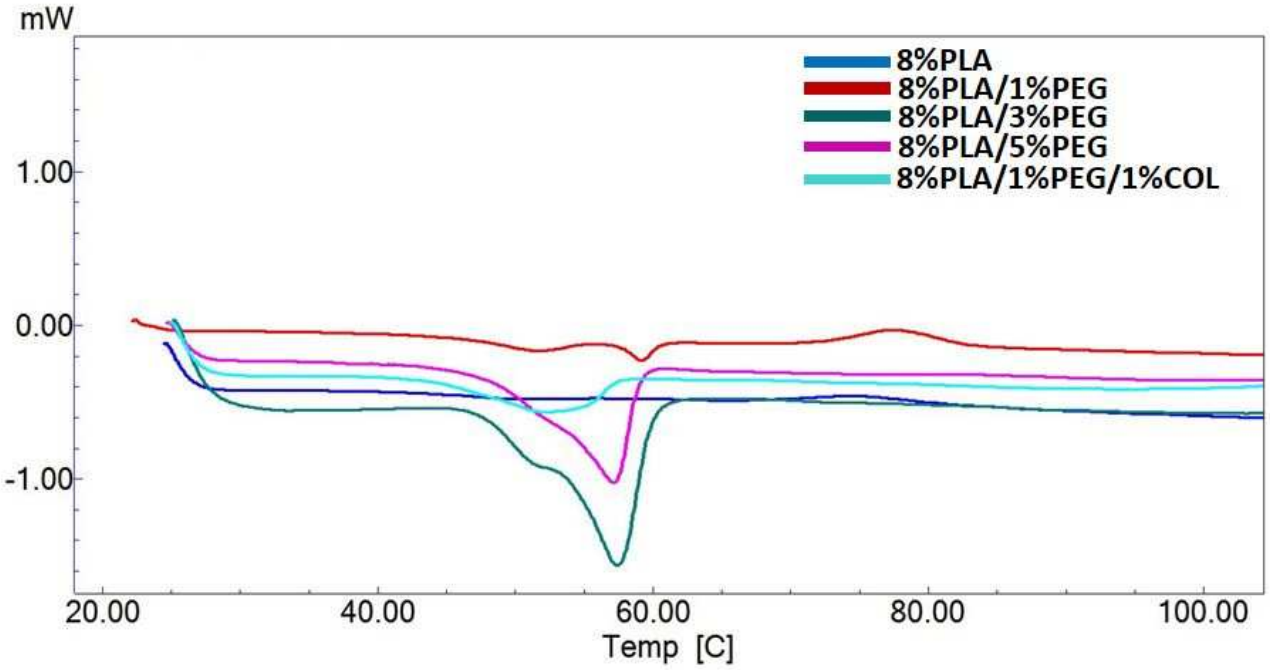

Figure 4. DSC thermographs of the nanofiber patches with their labels.

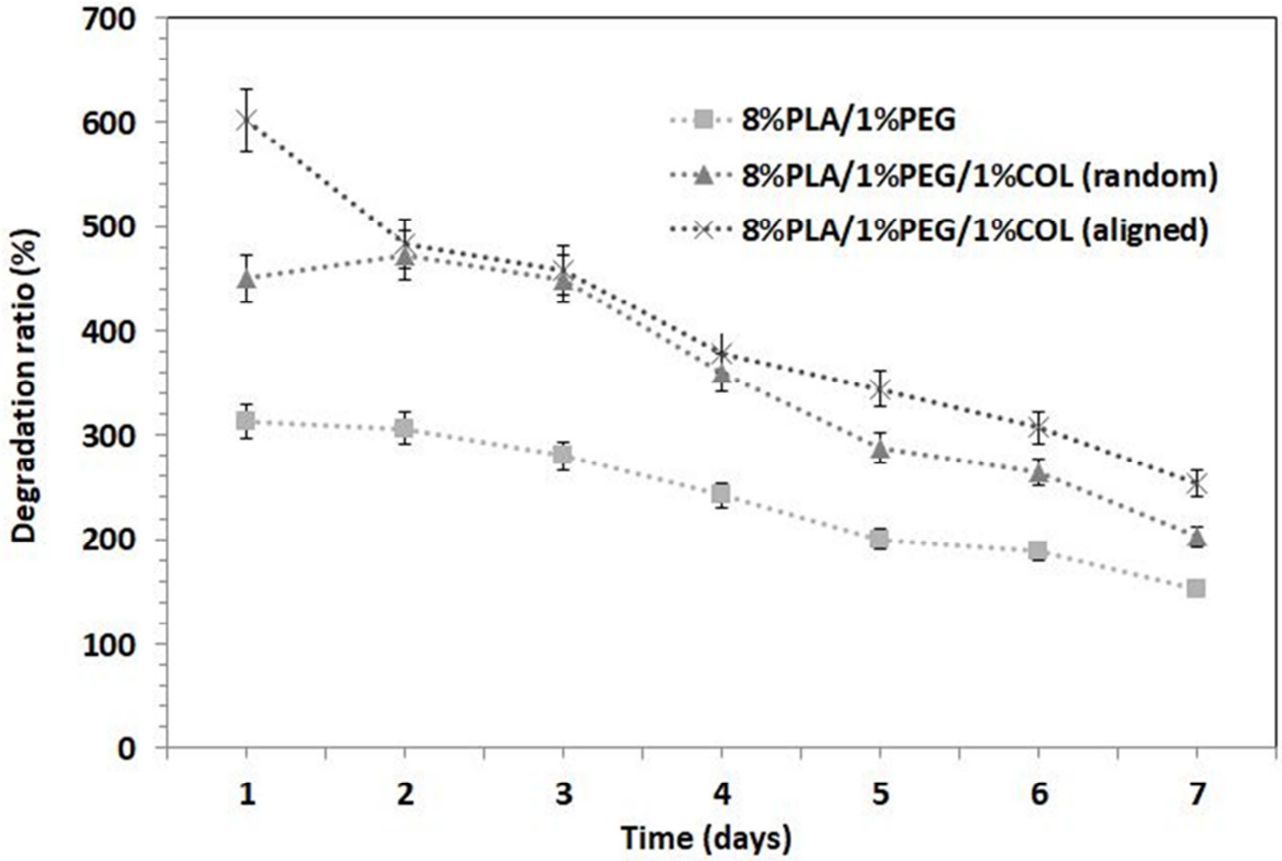

Figure 5. The degradation behaviours of the patches after 7 days of incubation.

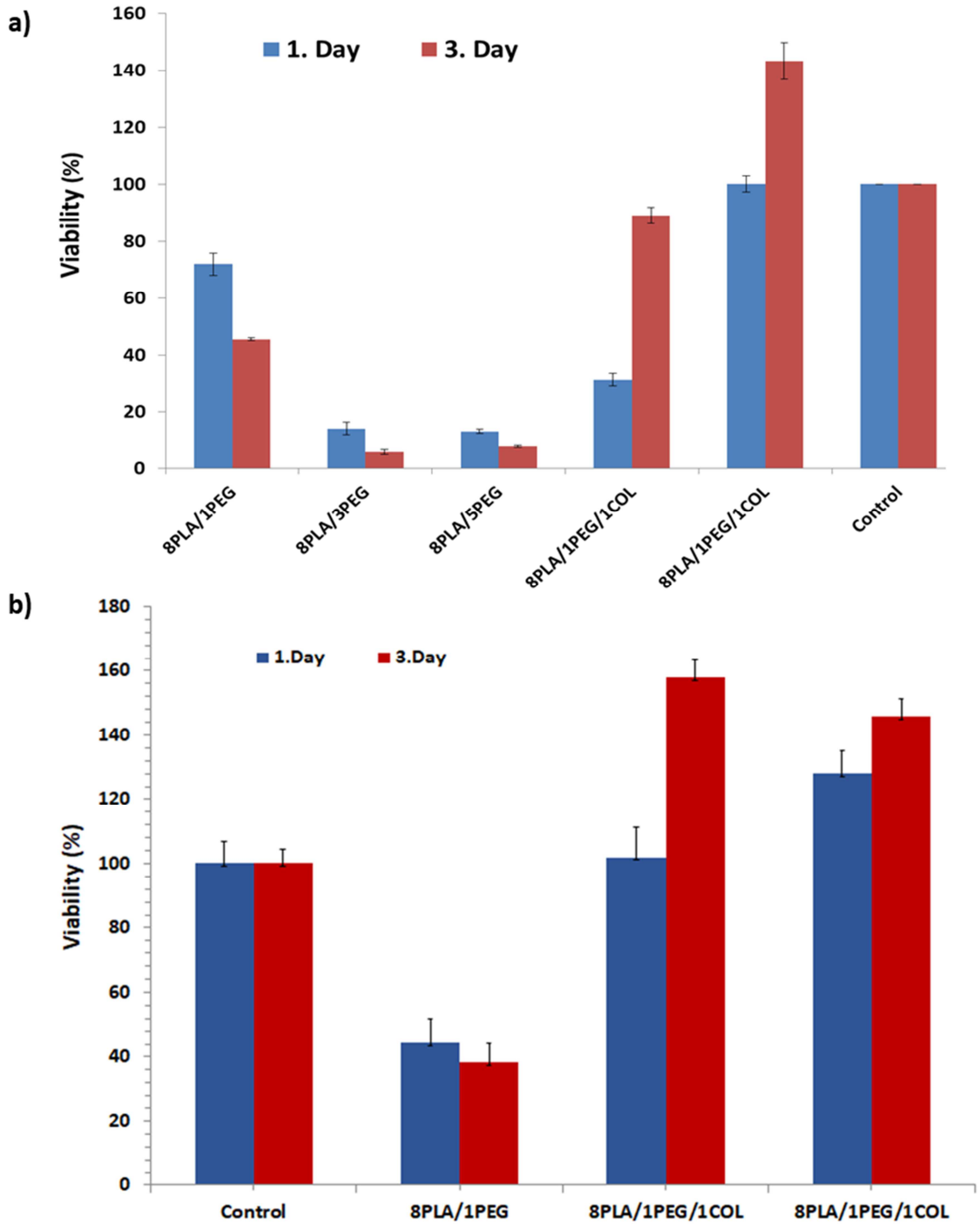

Figure 6. Cell viability graph of 2D H9C2 cells and nanofiber patches before (a) and after (b) degradation.

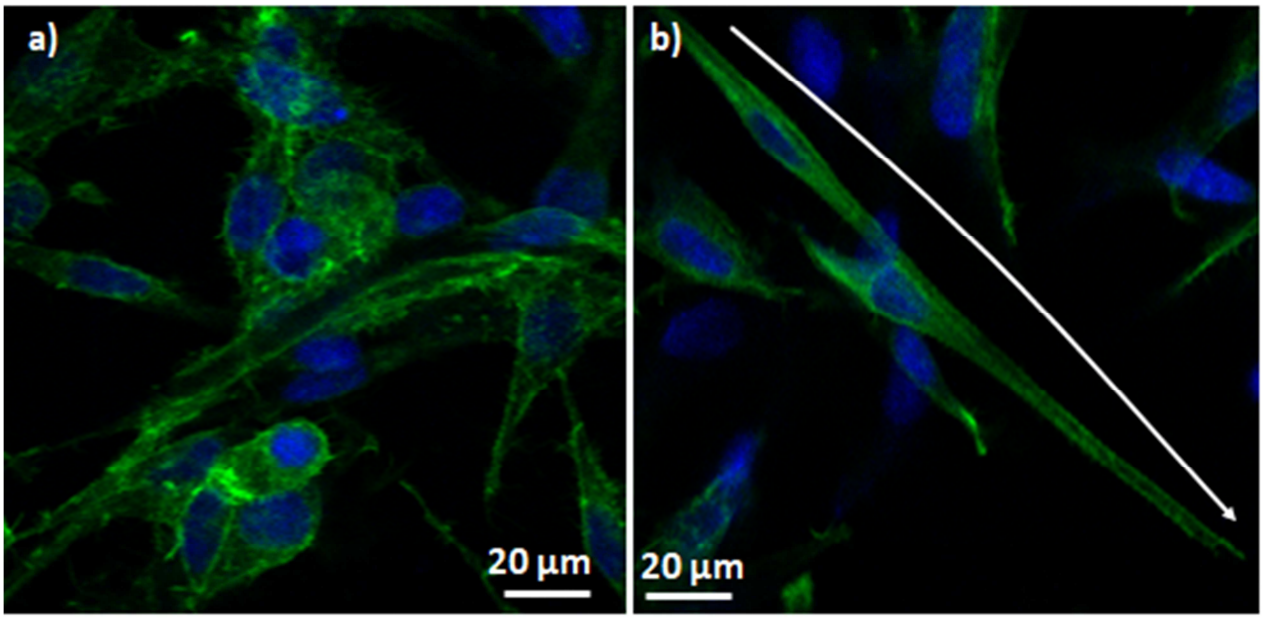

Figure 7. Confocal images of random (a) and aligned (b) 8%PLA/1%PEG/1%COL nanofiber patches.

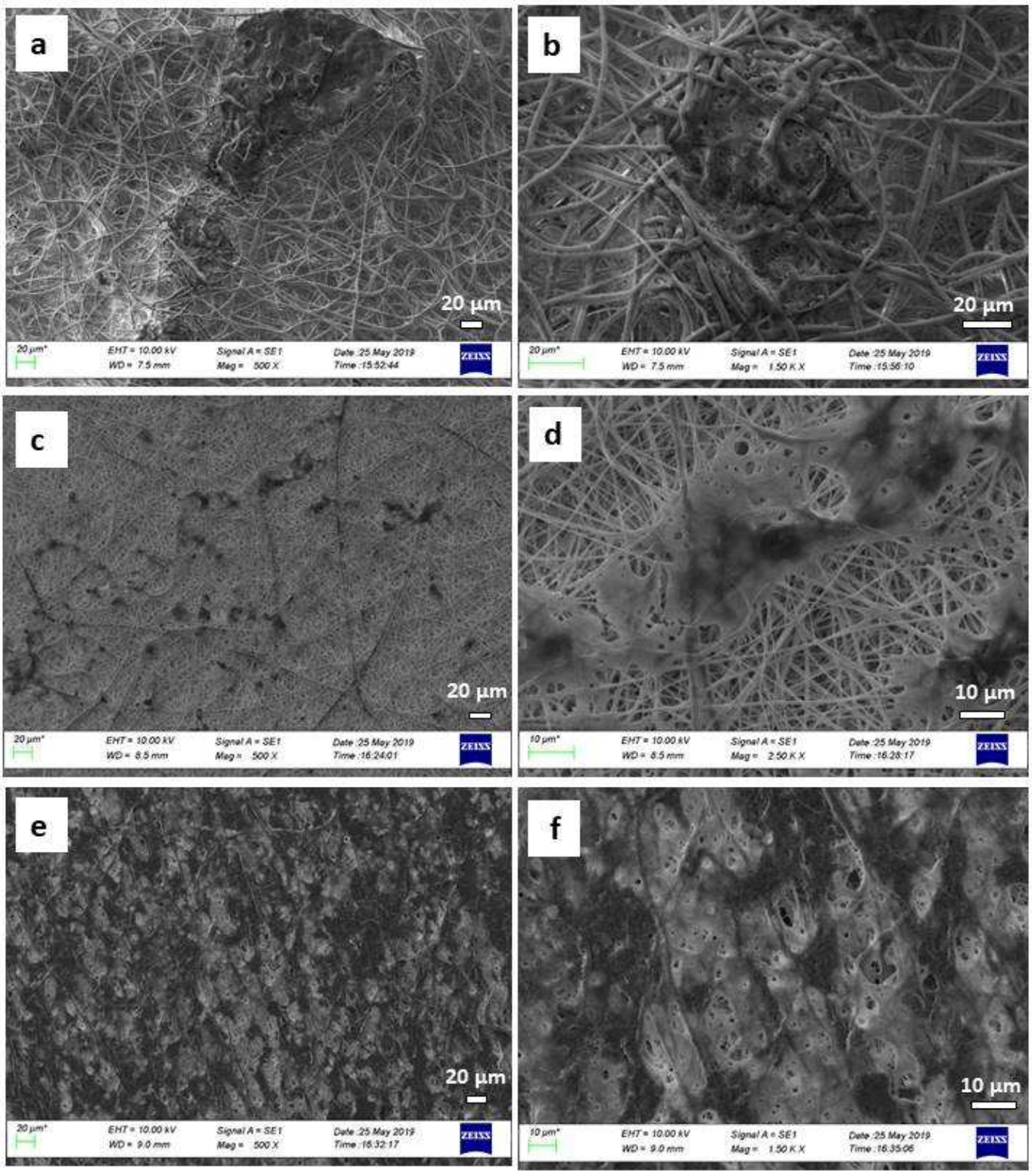

Figure 8. SEM images of H9C2 cells adhesion on patches with different magnifications, 8%PLA/1%PEG (a, b), 8%PLA/1%PEG/1%COL (random) (c, d), 8%PLA/1%PEG/1%COL (aligned) (e, f).

Table 1.

Nanofiber Patches	**PLA content (Wt %)**	**PEG content (Wt %)**	**COL content (Wt %)**	**Tween 80 (Wt %)**
8PLA	8	0	0	3
8PLA/1PEG	8	1	0	3
8PLA/3PEG	8	3	0	3
8PLA/5PEG	8	5	0	3
8PLA/1PEG/1COL (Random)	8	1	1	3
8PLA/1PEG/1COL (Aligned)	8	1	1	3

Table 2.

Concentration of Solutions	**Density (g/cm^3)**	**Electrical Conductivity (µS/cm)**	**Surface Tension (mN/m)**	**Viscosity (mPa.s)**
8 wt. % PLA	1.400	1.2	28.54	56
8 wt. % PLA 1 wt.% PEG	1.488	0.8	29.01	732
8 wt. % PLA 3 wt.% PEG	1.478	0.9	29.45	644
8 wt. % PLA 5 wt.% PEG	1.470	1.0	29.67	625
8 wt. % PLA 1 wt. % PEG 1 wt.% COL	1.409	64.1	29.46	580

Table 3.

Nanofiber Patches	Tensile strength (MPa)	Strain at break (%)
8wt.%PLA	0.24 ± 0.06	61.17 ±0.74
8wt.%PLA/1 wt.%PEG	0.25 ± 0,03	142.48 ± 17.1
8 wt.%PLA/3 wt.%PEG	0.11 ± 0.008	187.89 ± 4.02
8 wt.%PLA/5 wt.% wt.%PEG	0.10 ± 0.02	192.56 ± 8.47
8wt.%PLA/1wt.%PEG/1 wt.%COL (Random)	0,11 ± 0.01	72,13 ± 2.46
8wt.%PLA/1wt.%PEG/1 wt.%COL (Aligned)	5.90 ± 4.00	84.08 ± 11.76

Highlights

1. The PLA/PEG/Collagen nanofiber patches were produced successfully by using the electrospinning method both random and aligned orientation.
2. The high speed of the collector affected the nanofiber orientation by changing from random to aligned structures.
3. The high amount of PEG had a toxic effect on the cardiomyocyte cell line (H9C2).
4. Aligned nanofiber patches showed superior tensile strength value compared to the random nanofiber.
5. The effect of aligned structure on cardiomyocyte cell behavior observed efficiently.

Oguzhan Gunduz: Conceptualization, Methodology, Investigation **Sumeyye Cesur:** Methodology, Investigation, Experiment, Draft preparation **Songul Ulag:** Methodology, Investigation, Experiment, Draft preparation **Lara Ozak:** Experiment, Investigation **Aleyna Gumussoy:** Experiment, Investigation **Sema Arslan:** Cell culture experiment, Investigation **Betul Karademir Yilmaz:** Cell culture experiment, Investigation, Visualization **Nazmi Ekren:** Methodology, Investigation **Mehmet Agirbasli:** Investigation, Visualization, Reviewing and Editing **Deepak M. Kalaskar:** Reviewing and Editing.

Declaration of interests

☒ The authors declare that they have no known competing financial interests or personal relationships that could have appeared to influence the work reported in this paper.

☐The authors declare the following financial interests/personal relationships which may be considered as potential competing interests: